VTT Technical Research Centre of Finland

Effect of software implementation on the result of computational fluid dynamics simulation of circulating fluidized bed risers

Nikku, Markku; Niemi, Timo; Kallio, Sirpa; Daikeler, Alexander

Published in:
Engineering Reports

DOI:
10.1002/eng2.12460

Published: 01/02/2022

Document Version
Publisher's final version

Received: 26 May 2021 | Revised: 6 September 2021 | Accepted: 10 September 2021

DOI: 10.1002/eng2.12460

RESEARCH ARTICLE

Engineering Reports Open Access WILEY

Effect of software implementation on the result of computational fluid dynamics simulation of circulating fluidized bed risers

Markku Nikku[1] | **Timo Niemi**[2] | **Sirpa Kallio**[2] | **Alexander Daikeler**[3]

[1]School of Energy Systems, LUT University PL 20, Lappeenranta, Finland

[2]Process Modeling, VTT Technical Research Centre of Finland, Ltd., Espoo, Finland

[3]Institute for Energy Systems and Technology, Technische Universität Darmstadt, Darmstadt, Germany

Correspondence
Markku Nikku, LUT University PL 20, FI-53851 Lappeenranta, Finland
Email: mnikku@lut.fi

Abstract

While in scientific literature much focus is directed toward model validation, comparison, and even parametric investigations on individual model parameters, the possible effects of the used computational fluid dynamics (CFD) software on the results are largely neglected. In this article, CFD modeling of circulating fluidized beds (CFB) are performed with Ansys Fluent and OpenFOAM to investigate the effect of software implementation on the simulation results. Transient Eulerian–Eulerian simulations are performed of two different laboratory-scale CFB cold models in turbulent and circulating fluidized bed conditions. The same mesh and as identical models and settings as possible are utilized on both software. The obtained time-average profiles of pressure, velocity, and solids volume fraction are compared between the software and with available measurements. A difference in the granular energy equation was identified between the software, and a modification was made to achieve the same formulation. The effect of boundary conditions was also investigated. It was found that depending on the case, the software could have a notable effect on the results. These differences are found especially in particle distribution, visible in the vertical pressure and solids volume fraction profiles as well as in external circulation mass flow rates.

KEYWORDS

CFB, CFD, software implementation

JEL CLASSIFICATION

Chemical engineering

1 | INTRODUCTION

Increased computational capacity of computers has led to an increase in the utilization of different modeling tools in the simulation of various devices and systems. Numerical modeling is a cheap alternative to test new concepts and designs, compared to building prototypes, especially of large and expensive devices. Considering circulating fluidized bed (CFB) reactors and furnaces, where multiphase flow, heat transfer, and thermochemical reactions can occur simultaneously

in various time- and length scales with strong coupling, detailed and extensive measurements are hard and very time consuming to perform.[1] Fluidized beds are multiphase systems where particulate matter called the bed material is set to a fluidlike state by a fluid flow, and the fluidization regime of the system depends primarily on the fluid flow rate, reactor geometry, and fluid and bed material properties. In CFBs the fluid flow rate is high and the process is characterized by a strong internal circulation of the bed material within the riser and external circulation of particles leaving and returning to the reactor after separation from the fluid. However, modeling can provide significantly more insight into the behavior of these systems, especially if measurement possibilities are limited. Reliable modeling requires the utilization of validated and tested modeling approaches and models, thus measurements are crucial for model validation and development. The validation material is often obtained from smaller laboratory-scale devices specifically built for this purpose and equipped with several measurement ports. Thus, by first modeling these laboratory-scale devices, indications of the validity and applicability of different numerical modeling approaches and models can be obtained.

There are several approaches to modeling CFB reactors with computational fluid dynamics (CFD). From very detailed and computationally heavy discrete element method (DEM), more affordable Lagrangian particle grouping methods, such as multiphase particle-in-cell method (MP-PIC), to the so-called two-fluid method, where both the fluid and the solid phase are treated as Eulerian phases. For Eulerian methods, suitable closures are required for describing the behavior of the solid particles in a continuum model. Such closures are provided by the kinetic theory of granular flows.[2–4] Currently, there are several software available for modeling fluidized bed applications. Table 1 lists CFD software, which include either the kinetic theory of granular flows for the Eulerian solid phase and/or one or more Lagrangian approaches for description of the particulate phase. This list excludes many in-house software and cannot be considered exhaustive.

Many research papers can be found dealing with CFD modeling of CFB units with several approaches and here only a few examples are listed. Panday et al.[19] presented results of blind modeling of NETL laboratory CFB unit with the height of 15 m and diameter of 0.3 m. The simulations methods were Eulerian–Eulerian in 2D, in 3D with coarse and fine mesh, and Eulerian–Lagrangian with two different particle counts. From the comparison of simulation results with measurements, it was difficult to say what method or settings would be the most accurate as all methods showed large variations from the measurements. Zhong et al.[20] simulated a laboratory-scale CFB unit ($H = 1.8$ m and $D = 0.125$ m) with a 3D Eulerian–Lagrangian method and included combustion reactions. Wang et al.[21] utilized Barracuda VR in 3D simulation of a CFB unit ($H = 3.0$ m and $D = 0.40$ m). They compared their results with 2D Eulerian–Eulerian simulations by Niemi,[22] which utilized a particle size distribution, and reported better accuracy and lower demand for computational resources. Shi et al.[23] studied different exit geometries in a 3D CFB riser ($H = 3.0$ m and $D = 0.15$ m) with Barracuda VR. Zhang et al.[24] utilized MP-PIC method in pseudo-3D simulation of two CFB risers with MFIX with particle size distributions. Zeneli et al.[25] utilized Ansys Fluent with EMMS approach in 3D modeling of CFB carbonator pilot ($H = 8.661$ m and $D = 0.59$ m) with limestone reactions.

There are several studies presented in the literature, which compare results obtained with different modeling approaches, models, and parameter values within a model using the same CFD software.[26–31] The purpose of these studies is typically model validation and hence conclusions are drawn on the suitability of different modeling approaches, submodels, and parameter values for simulation of a specific type of application or flow condition. However, the implementation of these models in the software and the overall architecture of the software itself can also have effects on the result which has so far been largely ignored in model validation studies. This could lead to cases where one software offers

TABLE 1 Software for 3D CFD simulation of fluidized beds

Software	Methods	Reference
Ansys Fluent	E–E, E–L, DDPM[a], DEM	5
Ansys CFX	E–E, E–L	6
Barracuda VR	MP-PIC	7,8
MFIX	E–E, E–L, MP-PIC, DEM	9–11
OpenFOAM	E–E, E–L, MP-PIC, DEM	12–14
TransAT	E–L	15
Star-CCM+	E–E, E–L, DEM	16–18

Abbreviations: E, Eulerian; L, Lagrangian.
[a] DDPM in Fluent is similar to MP-PIC method.

excellent correspondence with the measured results while less satisfactory correspondence is obtained with another software using the same models. Only a few works can be found comparing different software for the same simulation case; for example, Mackenzie et al.[32] compared Ansys Fluent 15, Star-CCM+ 10.02, and OpenFOAM 2.3.x in modeling of a submerged jet and obtained very similar velocity profiles, López et al.[33] compared Ansys Fluent 15 and OpenFOAM 2.2.x with Lagrangian–Eulerian jet impingement erosion with results having minor discrepancies between the software, and Balogh et al.[34] compared Ansys Fluent 13 with OpenFOAM to study atmospheric boundary layer, finding some parameters better predicted by Fluent and others by OpenFOAM. Herzog et al.[11] compared Ansys Fluent 6.3, MFIX, and OpenFOAM 2.0 in modeling a benchmark bubbling fluidized bed. Their results show some differences between the software and they concluded that while MFIX and Fluent predicted fluidization phenomena well, OpenFOAM simulations required further efforts for the particular case. A similar study was performed more recently by Venier et al.[35] In Herzog et al.[11] and Venier et al.[35] the BFB simulation results were different depending on the software.

As many different CFD software exist, it is necessary to evaluate whether the selection of simulation software has an influence on the simulation results when the same computational mesh, boundary conditions, models, and simulation parameters are used. It is often assumed that with the same set of equations and similar modeling scheme the CFD results must be the same regardless of the software used, and the possible effects of the actual numerical implementation of the equations and their iterative solution process are not considered. It is relevant to challenge this assumption as the CFD software (a) are complex and (b) they are utilized in research and development where small differences could have a large influence on the bigger picture. The effects of this assumption are especially relevant in model validation and model parameter studies, where differences in the results from different software could render the results of such studies inconclusive or even contradictory between different software. In this article, the possible effects of the CFD software on the simulation results of CFB units are studied in turbulent and circulating fluidized bed conditions. Ansys Fluent 19.2[5] and OpenFOAM[12] with the solver reactingTwoPhaseEulerFoam[36,37] are utilized in transient Eulerian–Eulerian modeling of two different laboratory-scale cold models of CFB risers. The objective of the article is to investigate the effect of software on the simulation results when the computational mesh, simulations models, parameters, and boundary conditions are set to match as closely as possible between the CFD software. The effect of boundary conditions is also investigated. The time-averaged profiles of pressure, velocity, and solids volume fraction are compared between the CFD software as well as with the available measurements from the laboratory devices.

2 | EXPERIMENTAL METHODS

2.1 | Pseudo-2D CFB

The first set of measurements were done in a pseudo-2D laboratory-scale CFB device, also used previously by Mondal et al.,[38] pictured in Figure 1 along with the computational domain. The riser part of the device has a rectangular geometry with a height of 3 m, width of 0.4 m, and thickness of 1.5 cm. In the test case, the device was loaded with spherical glass beads with a material density of 2480 kg/m^3 and Sauter mean diameter of 255 μm. The device was operated at ambient temperature and pressure. The superficial fluidization velocity of air was 2.25 m/s which is below the velocity of 2.8 m/s above which according to Bi et al.[39] fast fluidization state is reached. Thus, the flow state in the riser during the experiment could be classified as turbulent fluidization although due to the fairly low riser height, 3 m, significant circulation of bed solids was observed. The total amount of glass beads was 2.68 kg and based on the amount of material in the loop seal, it was estimated that the average mass of solid particles in the riser during the experiment was 1.9 kg.

The device walls are transparent which allows optical measurements. Particle velocities were measured using particle image velocimetry (PIV). In this technique, the flow is recorded with a high-speed camera and the particle velocities are calculated based on the displacement of each particle in subsequent image frames and the time delay between the frames. In addition to velocity measurements, the instantaneous local concentration of particles was estimated from the gray-scale values of the image frames by using a logarithmic correlation function. Backlighting was used for these measurements. Overall, the measurement process was similar to what was used in Peltola et al.[40] who present the methodology in detail.

The PIV measurements were done at four different heights: 23, 40, 80, and 120 cm from the grid level. Unfortunately, for this experimental case, reliable pressure measurements were not available. The solids circulation rate was measured by turning off the airflow to the loopseal for a long enough period that allowed measuring the change in solid volume in the loop seal. The mass flow was then calculated using a measured bulk density of 1580 kg/m^3.

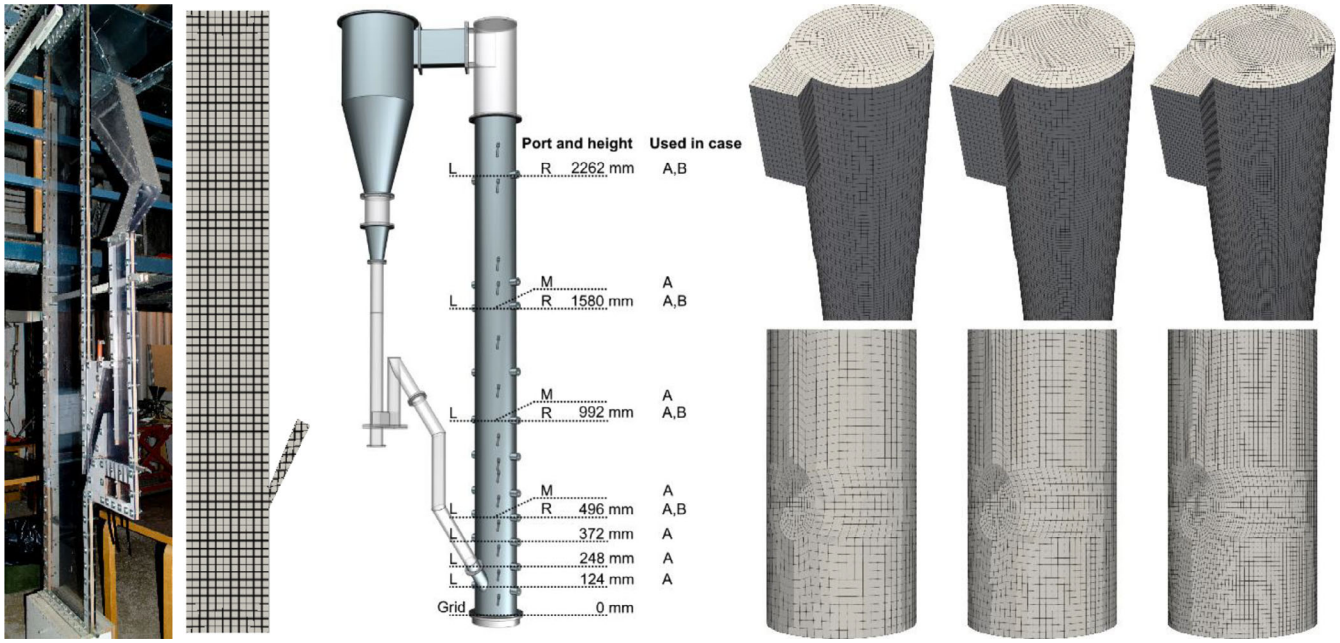

FIGURE 1 Geometries and used meshes of the pseudo-2D and cylindrical CFB risers

2.2 | Cylindrical CFB

The second set of measurements were conducted on a cylindrical laboratory-scale CFB device as described by Daikeler et al.[41] The riser has a diameter of 0.213 m and is 3.078 m high, with a schematic of the device presented in Figure 1. Several pressure measurement connections are placed along the height of the riser. Fluidization air for loopseal and the riser is delivered by a fan through a measurement orifice. The device was loaded with 9 kg of sand with material density of 2647 kg/m.[3] Density of air was approximately 1.2 kg/m^3 and viscosity $2.0{\cdot}10^{-5}$ m^2/s. The particle size and shape distributions of the glass beads were determined with 2D image analysis, with the volume average particle size being 193 μm. The sand particles can be considered spherical as the average measured circularity was relatively close to 1. The sand in the riser was fluidized with constant superficial velocity of 1.9 m/s in case A and 2.3 m/s in case B and in both cases 6 m^3/h of air fluidized the loop seal. Differential pressure transducers were used to measure the vertical pressure distribution and a capacitance probe was used to determine solids volume fraction and vertical velocity distributions inside the riser. More details on the probe measurements are found in Daikeler et al.[41] The external circulation mass flow rate of particles was measured by briefly stopping fluidization in the loopseal and measuring accumulation of particles in the return leg. The same measured cases have been previously simulated by Stroh et al.[42] with coarse-grained Eulerian–Lagrangian approach and Nikku et al.[43] with Eulerian–Eulerian approach.

3 | NUMERICAL METHODS

3.1 | Eulerian–Eulerian model

Eulerian–Eulerian two-fluid approach was used in simulation of the test devices. Equations 1 and 2 present the continuity equations and Equations 3 and 4 present the momentum conservation equations for the gas and the solid phase, respectively. The models utilized in the momentum conservation equation related to the kinetic theory of granular flow and the drag model are presented in Table 2 and Table 3, respectively.

$$\frac{d}{dt}(\alpha_g \rho_g) + \nabla \cdot (\alpha_g \rho_g \mathbf{u}_g) = \sum S_g, \tag{1}$$

$$\frac{d}{dt}(\alpha_s \rho_s) + \nabla \cdot (\alpha_s \rho_s \mathbf{u}_s) = \sum S_s, \tag{2}$$

$$\frac{d}{dt}(\alpha_g \rho_g \mathbf{u}_g) + \nabla \cdot (\alpha_g \rho_g \mathbf{u}_g \mathbf{u}_g) = -\alpha_g \nabla p + \nabla \cdot \bar{\tau}_g + \alpha_g \rho_g \mathbf{g} - K_{gs}(\mathbf{u}_g - \mathbf{u}_s) + \sum F_g + \sum S_{g,m}, \quad (3)$$

$$\frac{d}{dt}(\alpha_s \rho_s \mathbf{u}_s) + \nabla \cdot (\alpha_s \rho_s \mathbf{u}_s \mathbf{u}_s) = -\alpha_s \nabla p - \nabla p_s + \nabla \cdot \bar{\tau}_s + \alpha_s \rho_s \mathbf{g} + K_{gs}(\mathbf{u}_g - \mathbf{u}_s) + \sum F_s + \sum S_{s,m}. \quad (4)$$

In this article, two different software are applied in the simulations of the laboratory-scale CFB units described in the previous chapter. These are Ansys Fluent version 19.2 and reactingTwoPhaseEulerFoam-solver of OpenFOAM developmental version (build dev-16d810c5fe6c), with the developmental version used for the increased computational performance over the newest release versions (version 7) available during this article. Both software can utilize the kinetic theory of granular flows for Eulerian–Eulerian two-phase modeling. The objective of this article is to compare the simulation results of these software between each other and with available measurement data obtained from measurements of the two laboratory-scale experimental devices. Gas phase was modeled as laminar to ensure that turbulence model implementation has no effect on the results. Additionally, the gas phase turbulence was found to be significantly lower compared to velocity fluctuations due to gas–solid momentum exchange.[54,55]

The list of submodels and model parameters used for all simulation cases are listed in Table 4. The correspondence of the submodels was verified from Ansys Fluent manual and the source code of OpenFOAM with the selected models reportedly being identical. One notable difference between the software was found in granular energy equation. Ansys Fluent applies only the source term described by Lun et al.[45] (Equation 18), while an additional source term (Equation 19) is included in the original formulation of the reactingTwoPhaseEulerFoam-solver as described and discussed by van Wachen et al.[49] Thus, a comparison of OpenFOAM results with (original formulation) and without (modified formulation) Equation 19 are used to determine the effect of this parameter on the simulation results, as well as providing as similar models as possible between Ansys Fluent and OpenFOAM. van Wachen et al.[49] offer an extensive review of the submodels available for kinetic theory of granular flows, and should be referred for details on the models and their origins.

3.2 | Boundary conditions and model parameters

The cylindrical CFB riser was discretized to a structured computational mesh using Ansys ICEM CFD.[56] The average lengths of a cell side are 10, 8, and 6 mm and the meshes consist of 176,000, 321,000, and 745,000 hexahedral elements, respectively. The simulation parameters and boundary conditions were set to match the experimental values.

The mesh for the pseudo-2D CFB riser was made using the snappyHexMesh mesh generator that is included with OpenFOAM. The mesh primarily consists of hexahedral elements with a cell length of 5 mm. There is a small amount of nonhexahedral elements in the solids return channel. The total number of cells in this mesh is 146,700. Although the device was only 1.5 cm thick, a 3D mesh was used to include the effect of the front and back walls on the simulation. Although the mesh spacing exceeds in this case the unofficial rule-of-thumb limit of 10 times particle diameter, it was considered sufficient for this article that mainly focuses on comparing numerical software. Earlier Kallio et al.[57] found 5 mm mesh spacing to produce sufficiently mesh-independent results on Ansys Fluent for the same 255 μm sized particles when simulating the same pseudo-2D CFB in corresponding process conditions. The effect of refining the 5 mm mesh spacing was tested on OpenFOAM, this information is presented as Appendix S1. The differences from the mesh refinement were found small enough to justify the use of 5 mm mesh spacing for this article.

The applied boundary conditions are presented in Table 5 for the pseudo-2D and cylindrical CFB units. The effect of the used boundary conditions should be very similar in both software, though there are slight differences and it is also difficult to estimate how the boundary conditions are implemented in Ansys Fluent since the source code is not available. In Ansys Fluent the gas inlet at the grid was modeled with a fixed volume fraction, whereas in OpenFOAM a zero gradient boundary condition was applied together with a velocity boundary condition interstitialInletVelocity which acknowledges the local volume fraction to ensure constant gas flow. This boundary condition combination is numerically more stable due to smaller gradients between the cell center and the boundary. The effect of these different boundary conditions was tested and the effects were limited only to the cells near the boundary. No slip boundary condition was applied to gas velocity on riser walls and the Johnson–Jackson[58] partial slip boundary condition on the walls for solid velocity and granular temperature. Additionally, the effect of the implementation of these boundary conditions was studied by comparing them with no slip and free slip boundary conditions. For pressure, a special boundary condition in OpenFOAM was used to ensures that the flux through a boundary equals the flux calculated by the velocity boundary condition, approximately equaling the zero gradient boundary condition used in Ansys Fluent. For recirculation of the elutriated

TABLE 2 The models used for the kinetic theory of granular flow

Phase stress–strain tensors

$$\tau_g = \alpha_g \mu_g (\nabla \mathbf{u}_g + \nabla \mathbf{u}_g^T) - \frac{2}{3}\alpha_g \mu_g (\nabla \cdot \mathbf{u}_g) I, \tag{5}$$

$$\tau_s = \alpha_s \mu_s (\nabla \mathbf{u}_s + \nabla \mathbf{u}_s^T) + \alpha_s \left(\lambda_s - \frac{2}{3}\mu_s\right)(\nabla \cdot \mathbf{u}_s) I. \tag{6}$$

Solid shear viscosity,[9,44]

$$\mu_s = \mu_{s,col} + \mu_{s,kin} + \mu_{s,fr}, \tag{7}$$

$$\mu_{s,col} = \frac{4}{5}\alpha_s \rho_s d_s g_{0,ss}(1 + e_{ss})\sqrt{\frac{\Theta_s}{\pi}}, \tag{8}$$

$$\mu_{s,kin} = \frac{\alpha_s \rho_s d_s \sqrt{\Theta_s \pi}}{6(3 - e_{ss})}\left[1 + \frac{2}{5}(1 + e_{ss})(3e_{ss} - 1)\alpha_s g_{0,ss}\right], \tag{9}$$

$$\mu_{s,fr} = \frac{p_{fr} \sin\phi}{2\sqrt{I_{2D}}}. \tag{10}$$

Granular bulk viscosity[45]

$$\lambda_s = \frac{4}{3}\alpha_s \rho_s g_0 (1 + e_s)\left(\frac{\Theta_s}{\pi}\right)^{0.5}. \tag{11}$$

Solid pressure[45]

$$p_s = \alpha_s \rho_s \Theta_s + 2\rho_s (1 + e_{ss})\alpha_s^2 g_{0,ss} \Theta_s. \tag{12}$$

Frictional pressure[46]

$$p_{fr} = \begin{cases} 0 & \alpha_s < \alpha_{s,f,min} \\ Fr\frac{(\alpha_s - \alpha_{s,f,min})^n}{(\alpha_{s,max} - \alpha_s)^p} & \alpha_s \geq \alpha_{s,f,min} \end{cases}, \text{where } Fr = 0.05, n = 2 \text{ and } p = 5, \alpha_{s,min} = 0.5. \tag{13}$$

Radial distribution function,[47] also[48]

$$g_{0,ss} = \left[1 - \left(\frac{\alpha_s}{\alpha_{s,max}}\right)^{\frac{1}{3}}\right]^{-1}. \tag{14}$$

Granular energy equation (Θ_s is granular temperature), after[49]

$$\frac{3}{2}\left(\frac{d}{dt}(\alpha_s \rho_s \Theta_s) + \nabla \cdot (\alpha_s \rho_s \mathbf{u}_s \Theta_s)\right) = (-p_s \bar{\bar{I}} + \bar{\bar{\tau}}_s) : \nabla \mathbf{u}_s + \nabla \cdot (k_{\Theta s} \nabla \Theta_s) - \gamma_{\Theta s} + \phi_{gs} + J_s. \tag{15}$$

Granular conductivity, Syamlal et al.[9]:

$$k_{\Theta s} = \frac{15 d_s \rho_s \alpha_s \sqrt{\Theta_s \pi}}{4(41 - 33\eta)}\left[1 + \frac{12}{5}\eta^2(4\eta - 3)\alpha_s g_{0,ss} + \frac{16}{15\pi}(41 - 33\eta)\eta \alpha_s g_{0,ss}\right], \eta = \frac{1}{2}(1 + e_{ss}). \tag{16}$$

Collisional dissipation of energy[45]

$$\gamma_{\Theta s} = \frac{12(1 - e_{ss}^2) g_{0,ss}}{d_s \sqrt{\pi}} \alpha_s^2 \rho_s \Theta_s^{\frac{3}{2}}. \tag{17}$$

Energy exchange between the gas and solid phase due to fluctuation of particle velocity[45]

$$\phi_{gs} = -3K_{gs}\Theta_s. \tag{18}$$

Energy exchange between the gas and solid phase from the fluctuating force exerted by the gas phase through the fluctuating velocity of the particles[49,50]

$$J_s = \frac{K_{gs} d_s (\mathbf{u}_g - \mathbf{u}_s)^2}{4\alpha_s \rho_s \sqrt{\Theta_s \pi}}. \tag{19}$$

TABLE 3 Gidaspow drag model[51] based on Ergun[52] and Wen and Yu[53]

$$K_{gs} = \frac{3}{4} C_D \frac{\alpha_s \alpha_g \rho_g |\mathbf{u}_g - \mathbf{u}_s|}{d_s} \alpha_g^{-2.65} \quad , \quad a_g > 0.8. \tag{20}$$

$$C_D = \begin{cases} \frac{24}{\mathrm{Re}}(1 + 0.15\mathrm{Re}^{0.687}) & \mathrm{Re} \leq 1000 \\ 0.44 & \mathrm{Re} > 1000 \end{cases}. \tag{21}$$

$$K_{gs} = 150 \frac{\alpha_s (1 - \alpha_g) \mu_g}{\alpha_g d_s^2} + 1.75 \frac{\alpha_s \rho_g |\mathbf{u}_g - \mathbf{u}_s|}{d_s} \quad , \quad a_g \leq 0.8. \tag{22}$$

TABLE 4 List of the utilized models

	OpenFOAM	Ansys Fluent
Gas–solid drag	GidaspowErgunWenYu, Equations 20–22	Gidaspow, Equations 20–22
Lift	No	No
Granular pressure	Lun, Equation 12	lun-et-al., Equation 12
Granular temperature	Equation 15	Equation 15
Granular conductivity	Syamlal, Equation 16	syamlal–obrien, Equation 16
Granular viscosity	Syamlal, Equations 8 and 9	syamlal–obrien, Equations 8 and 9
Granular energy source terms	Original: Equations 18 and 19 Modified: Equation 18	Equation 18
Bulk viscosity	Lun et al., Equation 11	lun-et-al., Equation 11
Frictional viscosity	Schaeffer, Equation 10	schaeffer, Equation 10
Angle of internal friction	28.5	28.5
Frictional pressure	JohnsonJackson, Equation 13	johnson-et-al., Equation 13
Frictional packing limit	0.5	0.5
Solids pressure	Equation 12	lun-et-al., Equation 12
Radial distribution	SinclairJackson, Equation 14	lun-et-al.,[a] Equation 14
Virtual mass	No	No
Collisions	bed-bed 0.8	bed-bed 0.8
Surface tension	No	No

Note: The model names and parameters are presented as they appear in each software for reproducibility.
[a]The naming in Ansys Fluent is misleading, while the equation is correct.

particles, a closure was implemented to keep the mass of the system constant using a user defined function (UDF) in Ansys Fluent, and a custom boundary condition in OpenFOAM. The air volume fraction is computed as unity minus the particle volume fraction. With both software, the cases were simulated assuming constant gas density and temperature equal to the measured ambient values.

3.3 | Simulation settings

For OpenFOAM, Courant number controlled adaptive time stepping was used with a maximum allowed Courant number of 1.0 and maximum time step $5{\cdot}10^{-4}$ s. For Ansys Fluent, it is not possible to use adaptive time-stepping with Eulerian–Eulerian multiphase simulations,[5] therefore cases were run with fixed time steps of $5{\cdot}10^{-4}$ s. Due to different approaches in the handling of time-step size and solution routines, which also significantly affects the simulation times, the comparison of the simulations times between the software is not representative and is not presented. Discretizations of the solved equations are presented in Table 6. OpenFOAM offers more control over the discretization of different parameters, while Ansys Fluent only allows for spatial, temporal, and gradient discretization to be selected. For both software, a first order accurate method was used for time discretization, a second order accurate method for spatial discretization, and central differencing was used for gradients. After initialization and development of quasi-steady multiphase flow, at least 30 seconds was simulated for time-averaging.

TABLE 5 The boundary conditions for the pseudo-2D and cylindrical CFB cases

		α_s [−]	u_s [m/s]	u_g [m/s]	p [Pa]	θ [m²/s²]
Grid	OF	zeroGradient	uniform (0 0 0)	interstitialInletVelocity p2D: 2.25 cyl: 1.9 / 2.3	fixedFluxPressure	zeroGradient
	AF	0	velocity-Inlet, 0	velocity-inlet p2D: 2.25 cyl: 1.9 / 2.3	Initial gauge pressure 0	1e-4
Solids return	OF	Custom	surfaceNormalFixedValue p2D: 0.4 cyl: 0.1	surfaceNormalFixedValue p2D: 0.1 cyl: 0.167	fixedFluxPressure	1e-4
	AF	UDF	Velocity-Inlet p2D: 0.4 cyl: 0.1	velocity-Inlet p2D: 0.1 cyl: 0.167	Initial gauge pressure 0	1e-4
Outlet	OF	zeroGradient	zeroGradient	zeroGradient	pressureInletOutletVelocity	zeroGradient
	AF	-	-	-	pressureOutlet, gauge pressure 0	-
Walls: Johnson–Jackson	OF	zeroGradient	JohnsonJacksonParticleSlip, specularity 0.01	noSlip	fixedFluxPressure	JohnsonJacksonParticleTheta, specularity 0.01, restitution 0.9
	AF	-	Specularity coefficient 0.01	no slip	-	Johnson-Jackson, restitution coefficient 0.9
Walls:free slip	OF	zeroGradient	Slip	noSlip	fixedFluxPressure	zeroGradient
	AF	-	Specified Shear 0	no slip	-	Specified flux 0
Walls: no slip	OF	zeroGradient	noSlip	noSlip	fixedFluxPressure	zeroGradient
	AF	-	noSlip	no slip	-	Specified flux 0

Note: The boundary condition models and selections are presented as they appear in each software for reproducibility, OF refers to OpenFOAM, AF to Ansys Fluent, p2D to pseudo-2D, and cyl to cylindrical. For walls, three different boundary conditions are investigated: Johnson–Jackson, free slip, and no slip.

TABLE 6 Discretization schemes used in the simulations, reported for reproducibility

	OpenFOAM			Ansys Fluent
	Scheme	**Model name**	**Accuracy**	
Time derivatives	ddtSchemes	Euler	First order implicit	First order implicit
Gradients	gradSchemes	Gauss linear	Central differencing	Least squares cell based—weighted central differencing
Surface normal gradients	snGradSchemes	uncorrected	Second order accurate	
Divergence operators	divSchemes	Gauss vanLeer/Gauss limitedLinear/Gauss limitedLinear V	Second order with varying degree of limiting toward upwind	Second order accurate
Laplacian operators	laplacianSchemes	Gauss linear uncorrected	Second order	
Cell to face interpolation	interpolationSchemes	linear	Central differencing	

4 | RESULTS

4.1 | Pseudo-2D results

4.1.1 | With Johnson–Jackson boundary conditions

The pseudo-2D case was simulated with Ansys Fluent and with OpenFOAM both with the additional source term for granular energy (Equation 19, denoted by $+J_s$) and without this term (denoted by $-J_s$). Figures of instantaneous and

time-averaged solids volume fraction are presented in Appendix S1. The predicted vertical pressure profiles for the cases are presented in Figure 2. There is a significant difference between the results of Ansys Fluent and OpenFOAM. Compared to OpenFOAM results, in Ansys Fluent pressure gradient is larger in the lower part of the riser and smaller higher up indicating a denser bottom region and more dilute upper part of the riser. On the other hand, the difference between the two OpenFOAM cases is practically negligible. Unfortunately, no pressure measurements were available for comparison.

Figure 3 compares the simulated solids volume fractions (A–D) and vertical velocities (E–H) with the measured values. The simulated profiles of volume fractions are similar at all levels, except for the 120 cm (Figure 3D), where Ansys Fluent profile is only approximately half of OpenFOAM values. The simulated volume fraction profiles provide a qualitatively good match with the measurement results near the walls, while significantly underestimating the volume fraction at the core. At the bottom of the riser (A), Ansys Fluent overpredicts the wall layer concentration and thickness, while the volume fraction at the core is similarly underpredicted by both software. Compared with the measurements, OpenFOAM better captures the wall layer gradient. As with the pressure profiles, the differences between the two OpenFOAM cases are very small. Considering that there are large differences in the pressure profiles, the volume fraction profiles are very similar between the two software at lower elevations, although Ansys Fluent clearly predicts higher solid concentrations.

The predicted solids velocity profiles (E–H) agree well with the measurements near the walls, while overpredict the velocity in the core. The agreement with the velocity measurements improves with height, with Ansys Fluent offering somewhat better agreement with the measurements at higher elevations (G and H) and OpenFOAM at lower elevations (F). The omission of the additional source term from the granular energy equation marginally improves the match between predicted and measured velocities. The discrepancies between the simulation results and measurements could be partly caused by the measurement setup as later explained.

The simulated solid circulation rates were 1.7 g/s for Ansys Fluent and 5.3 g/s for OpenFOAM with source term and 5.1 g/s without, all significantly below the measured rate of 21 g/s. However, in turbulent fluidization conditions prevailing in the riser, the circulation rate is an order of magnitude smaller than in fast fluidization conditions and both software correctly predict a low circulation rate. In turbulent fluidization conditions, even small deviations in particle size distribution and process parameters can have significant effects on the circulation rate and thus the large relative differences are not uncommon.

Some of the differences between the measurements and simulated results can be explained by deficiencies in the experimental and measurement process. Although the device was thin and the camera was focused on the middle plane of the device, slow-moving particles near the front wall can likely have some effect on the measured velocity profiles especially in the dense bottom region. Thus, it is quite likely that the measured velocity profiles are too flat in the bottom region and the velocity profile could have a more parabolic shape similar to the simulated results. Also, as explained by Peltola et al.,[40] it is quite difficult to calibrate the gray-scale volume fraction estimate to give quantitatively accurate predictions for the whole range from very dilute to fully packed conditions and instead, the volume fraction measurements should be taken more as a qualitative indicator. The measured volume fraction levels at 23 and 40 cm are almost identical (Figure 3A,B), while 80 and 120 cm levels (C,D) are quite high and most likely a bit overpredicted in the dilute regions

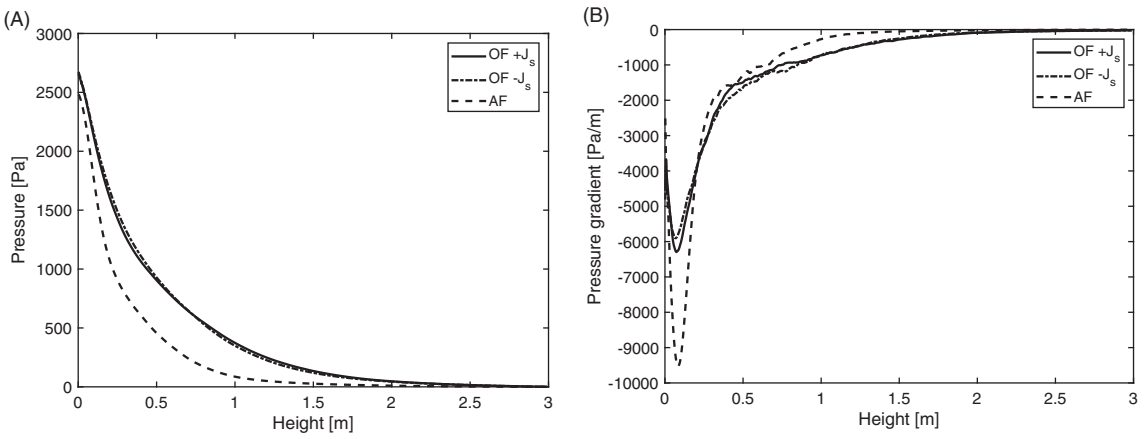

FIGURE 2 Centerline pressure (A) and pressure gradient (B) profiles in the pseudo-2D riser

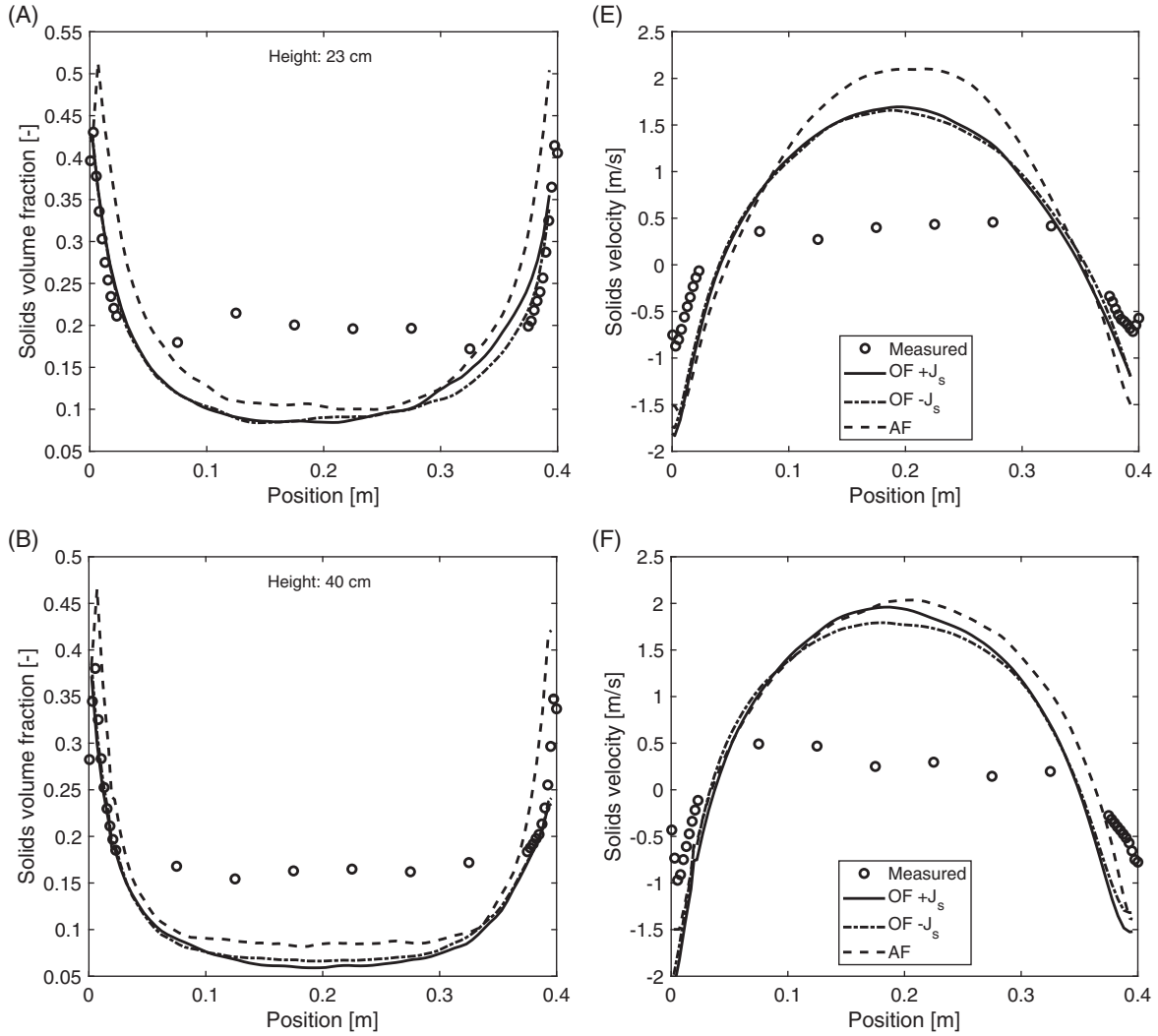

FIGURE 3 Solids volume fraction (A–D) and velocity (E–H) profiles compared with measurements from the pseudo-2D riser

at the core. This conclusion is supported by the fact that integration of the solid volume fraction field determined from video images results in clearly larger bed mass than what actually resides in the riser.

4.1.2 | Effect of wall boundary conditions

To investigate the effect of the wall boundary conditions on the simulation results, the pseudo-2D case was also simulated using both no slip and free slip boundary conditions for the solid velocity and zero gradient for the granular temperature. The primary motivation for this test was to see how the two software react when the reasonably complicated Johnson–Jackson boundary conditions are replaced with simpler boundary conditions. OpenFOAM with the modified formulation (with the J_s-term) was utilized in this comparison with Ansys Fluent. The results of this comparison are presented in Figures 4 and 5. While both software reacted to the changes in a qualitatively similar way, the response was stronger with Ansys Fluent than with OpenFOAM. Both software predicted denser bottom bed and lower upward velocities with no slip boundary condition and more dilute bottom bed and higher velocities with free slip condition compared to the Johnson–Jackson results. However, these changes were most visible at the very bottom, below the first measurement level. Higher up in the riser, the results with all boundary conditions were quite similar to each other in both software and there were no significant changes to the pressure profile or recirculation rates. Overall, the agreement between the two software did not significantly improve with simpler boundary conditions even though the qualitative response was similar. This suggests that the differences between the simulation results do not originate from the boundary conditions or their implementation.

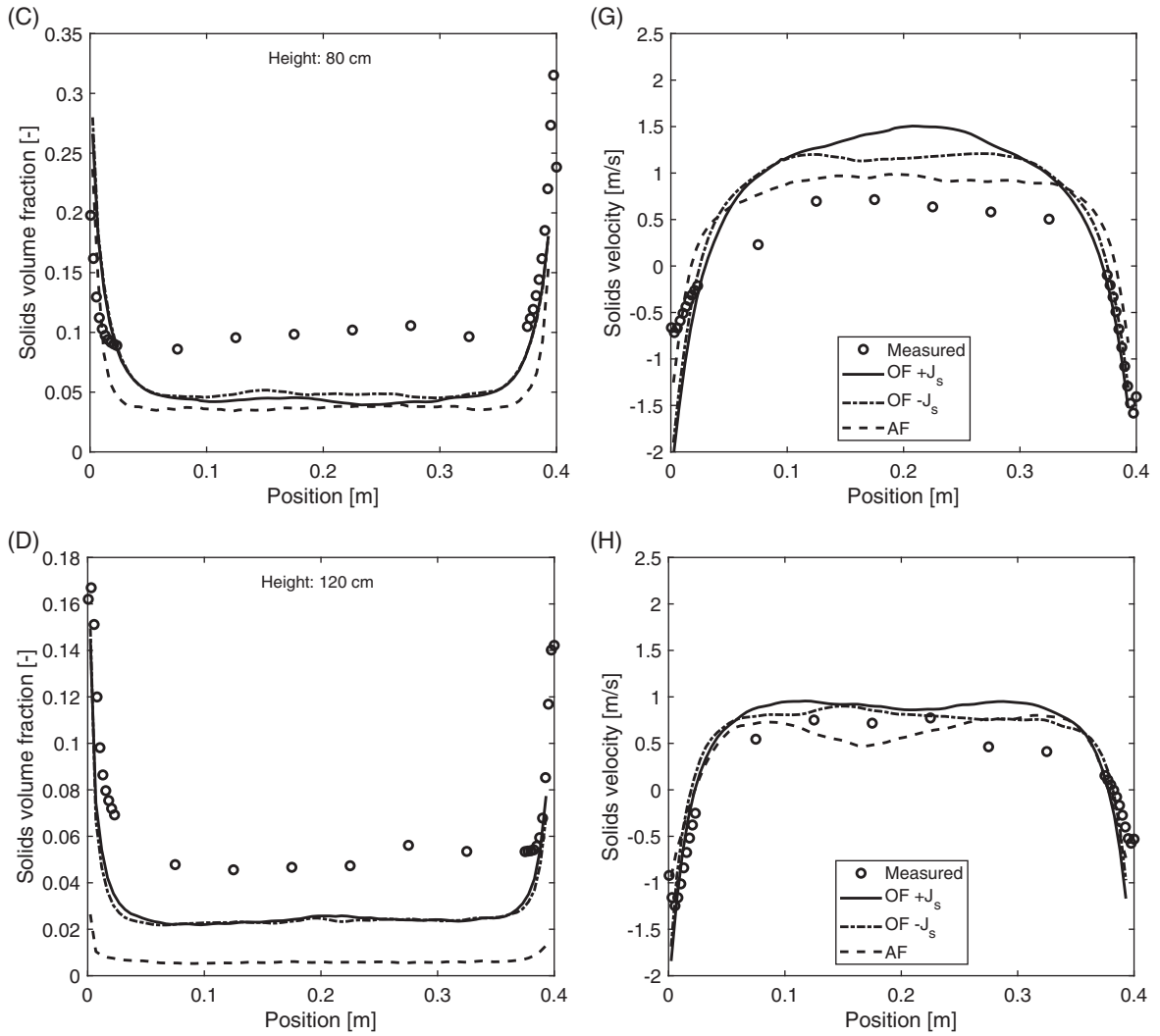

FIGURE 3 (Continued)

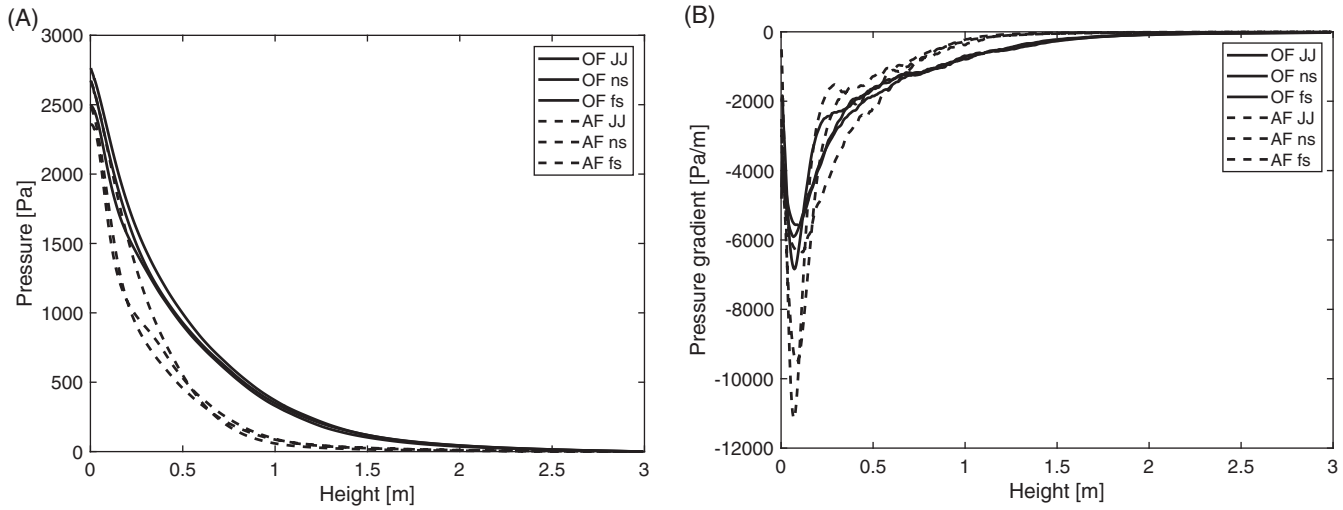

FIGURE 4 Comparison of pressure (A) and pressure gradient (B) profiles in pseudo-2D riser with (JJ) the Johnson–Jackson, no slip (ns), and free slip (fs) boundary conditions

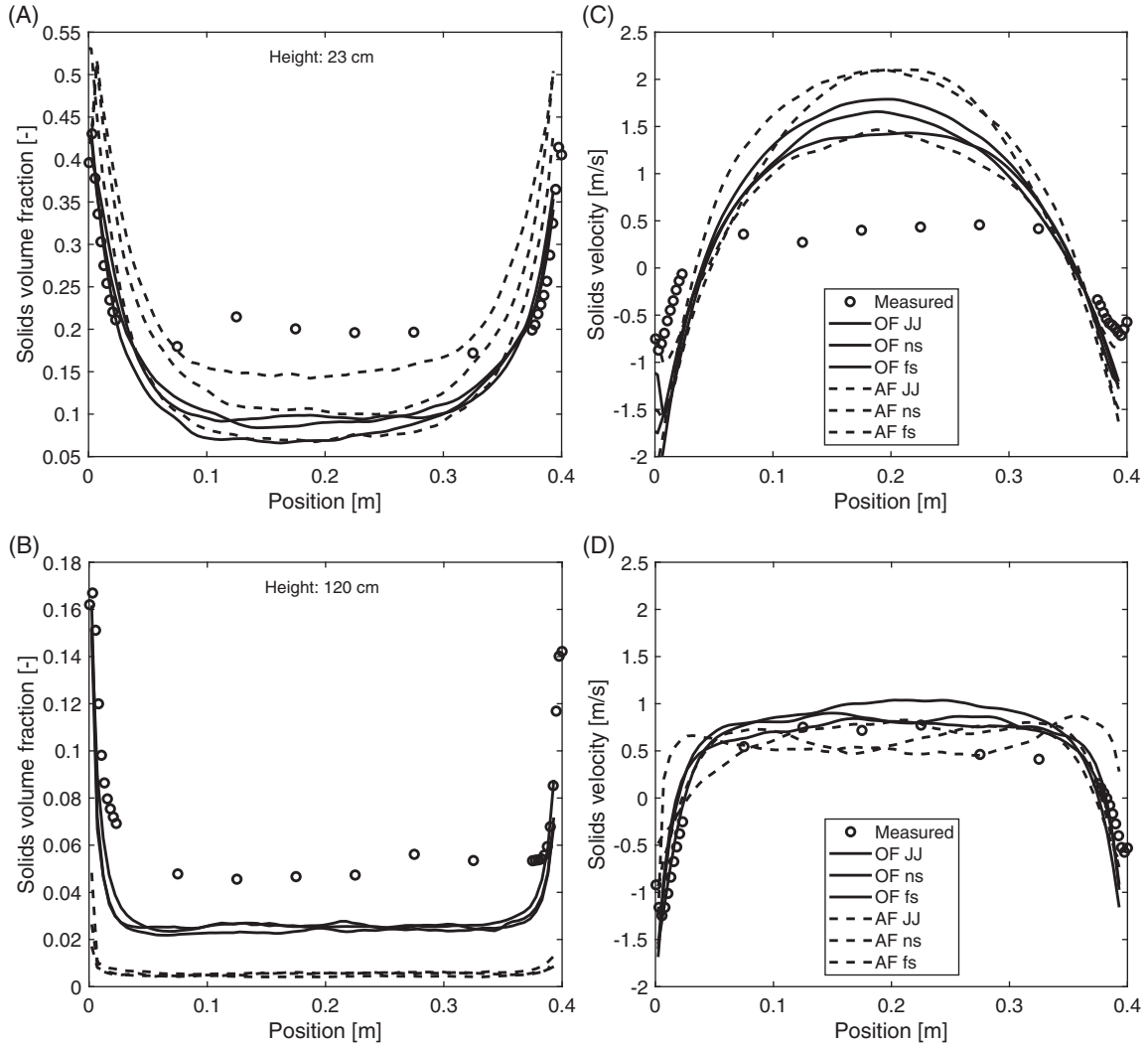

FIGURE 5 Comparison of solids volume fraction (A–B) and velocity (C–D) profiles compared with measurements from the pseudo-2D riser with (JJ) the Johnson–Jackson, no slip (ns), and free slip (fs) boundary conditions

4.2 | Cylindrical CFB

4.2.1 | Mesh independence

The mesh independence was evaluated by comparing the time-averaged simulated vertical pressure profiles as well as solids volume fraction and vertical velocity profiles. Figure 6 presents the pressure profiles for the simulated cases with different mesh sizes, which serves as an overview of the distribution of the solids inside the riser. The solids volume fraction and vertical velocity profiles as well as external circulation mass flow rates for different mesh sizes are presented as Appendix S1. Average differences in pressure between the 10 and 8 mm as well as 8 and 6 mm meshes were calculated. The differences between Ansys Fluent results with different meshes in case A were all well below 10%, which was considered the limit for a significant effect of the mesh, similarly to OpenFOAM with the modified formulation. The original OpenFOAM formulation showed approximately 15% change between 6 and 8 mm mesh sizes, with the 6 mm moving results closer to the modified formulation results. Comparison of external circulation mass flow rates, as well as the solids velocity and volume fraction profiles also indicated some differences between the mesh sizes. Local variation in the profiles is observed between different mesh sizes, while the trend and overall level of the volume fraction and velocity remain similar. The variations are larger in velocity and the relative differences are larger in the more dilute top parts of the riser. Based on these analyses, 6 mm mesh results are used in further comparison for all cases.

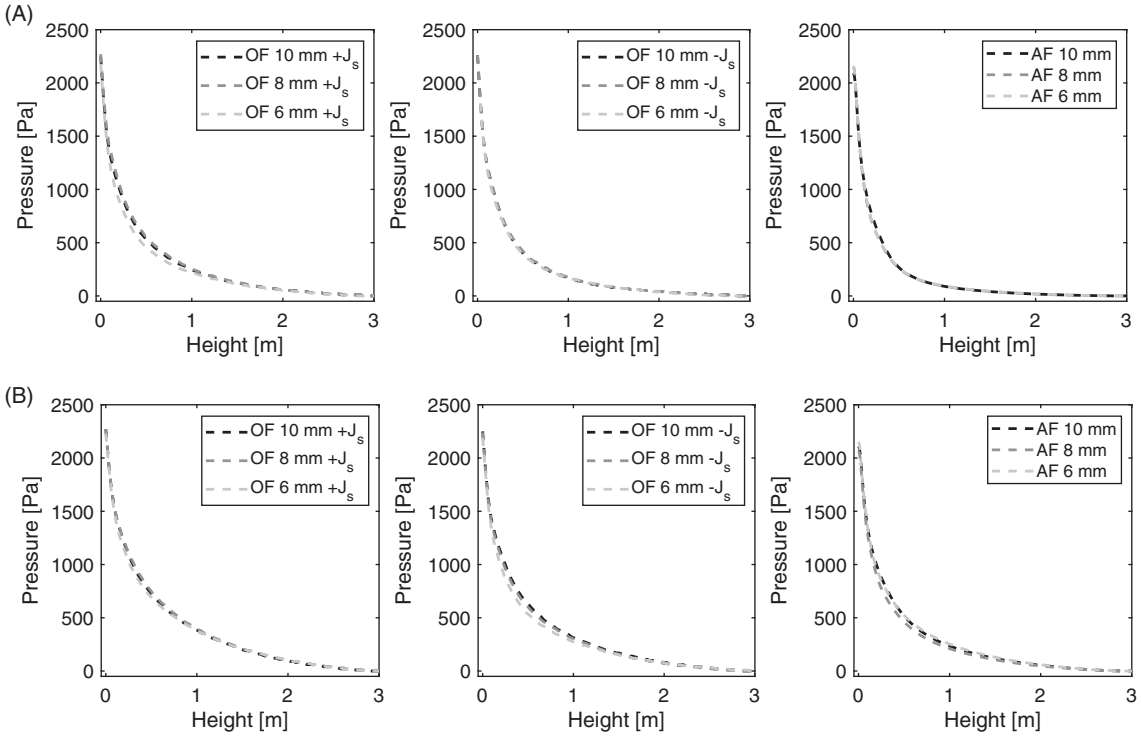

FIGURE 6 Vertical pressure profiles for (A) case A and (B) case B with different mesh sizes

TABLE 7 Average external circulation rates of particles with standard deviation

Case	Meas., st.dev [g/s]	AF	OF−J_s	OF+J_s
A	101, 4	35.4, 8.9	50.8, 11.3	71.6, 17.7
B	220, 11	163.6, 43.1	226.9, 48.9	344.4, 68.5

4.2.2 | External circulation mass flow rates

Table 7 presents the measured and modeled circulation mass flow rates. A significant difference is observed between the two OpenFOAM formulations. The original OpenFOAM (denoted by $+J_s$) results show significantly higher rates of external particle circulation compared to the modified OpenFOAM (denoted by $-J_s$) and Ansys Fluent. Compared to the measurements, Ansys Fluent significantly underestimates the external circulation rate in both cases. The modified OpenFOAM offers the best agreement with measurements in case B while underestimating the measurements in case A. The original OpenFOAM significantly overestimates the external circulation rates in case B while having the closest, somewhat underestimated results in case A.

Reasons for the differences between measured and modeled results are due to solids concentration and velocity profiles. Extrapolating based on the highest measurement level results (presented later), in case A the lower modeled solids velocities and higher volume fractions lead to a lower mass flow rate compared to the measurements. Similarly, for case B, the higher concentrations and similar velocities to the measurements would lead to higher mass flow rates. This is supported by the order of modeled volume fraction profiles at height 2262 mm in case A, while in case B, a combination of vertical velocity and volume fraction profiles could explain the differences especially between Ansys Fluent and the modified OpenFOAM.

4.2.3 | Vertical pressure profile

Figure 7 presents the modeled and measured vertical pressure profiles. The effect of the additional source term in the granular temperature equation on the OpenFOAM pressure profiles is clearly seen. In both cases, the original

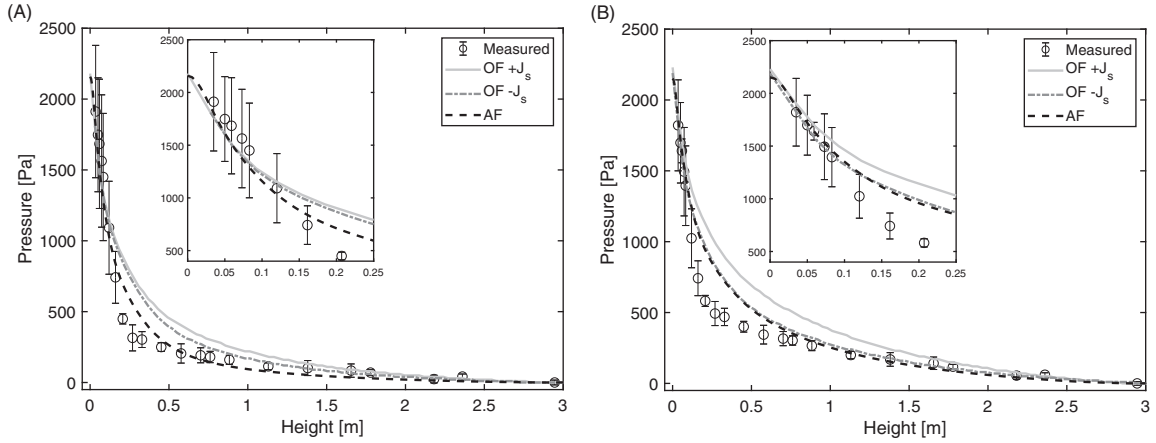

FIGURE 7 Pressure profiles compared with measurements on (A) the case A, and (B) the case B

OpenFOAM results show smaller pressure drops in the bottom and middle parts of the riser compared to both Ansys Fluent and the modified OpenFOAM. The modified OpenFOAM results are closer to Ansys Fluent results compared to the original OpenFOAM, with better correspondence in case B than in case A. Compared to the measurements, the modified OpenFOAM still predicts a smaller pressure gradient similar to the original OpenFOAM. Ansys Fluent results are in good agreement with the measurements, showing the least deviation. All simulations predict similar and correct pressure drop over the riser in both cases.

4.2.4 | Solids volume fraction and vertical velocity

Figures 8 and 9 present comparisons of solids volume fraction and vertical velocity profiles for case A and case B, respectively. Figures of instantaneous and time-averaged solids volume fraction are presented in Appendix S1.

For case A, at the bottom, all simulated solids velocities (Figure 8G–L) are very similar in level and profile shape. As the height increases, the correspondence near the wall remains good between the software, but velocities predicted by Ansys Fluent at the core are lower and underestimate the measured values. The OpenFOAM velocities are similar between the formulations, with the modified formulation having lower values at the core. OpenFOAM velocity results agree well with measurements in the middle parts of the riser (Figure 8H,I), while overestimating the measurements slightly at the bottom (G), and significantly underestimating at the higher levels (J–L). All simulation results match well with the measured wall layer velocities, except at the highest measurement levels, where the measured profiles show skewing, and at the lowest measurement level where simulations predict a falling wall layer not shown by measurements. Ansys Fluent appears to predict the change in the profile shape at the top of the riser (Figure 8L) while underestimating the core velocities on a level similar to OpenFOAM. For case B, the differences between the simulated results are similar to case A except that the modified OpenFOAM velocities are closer to Ansys Fluent velocities than the original OpenFOAM velocities. Ansys Fluent offers the closest match with the measured velocities in the middle parts of the riser (Figure 9 E,F) and even manages to predict the changed profile shape above 1580 mm level.

In case A, the simulated solids volume fraction levels (Figure 8A–F) are matching well at the bottom with all software (A–C), although the simulations produce a thinner and denser wall layer than what is shown in measurements. However, similarly to the pressure profile, the simulated results overpredict the solids volume fractions higher in the riser. In the lower part of the riser (A–C), Ansys Fluent and OpenFOAM results match well with each other up to 496 mm level, above which the simulated results start to separate from each other. At the highest measurement level (F), results of Ansys Fluent and the modified OpenFOAM match the measured volume fraction profiles, while original OpenFOAM results overestimate solids volume fraction. Simulations predict larger wall volume fraction gradients in the wall layer compared to the measurements, in which the profile shape is flattening as the height increases. In case B (Figure 9A–D), the results are similar to case A, but the modified OpenFOAM and Ansys Fluent results remain almost similar on

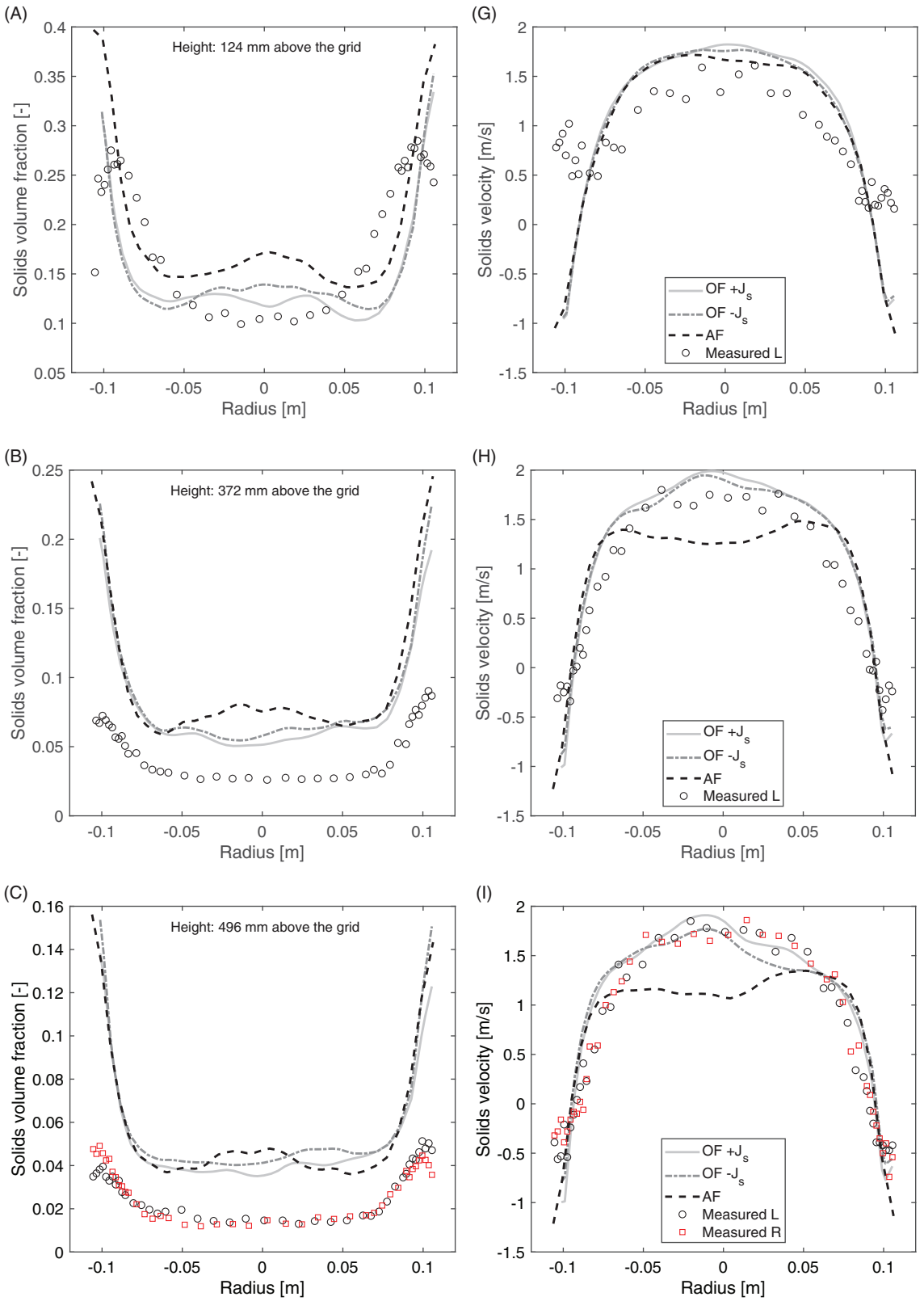

FIGURE 8 Profiles of solids volume fraction (A–F) and vertical velocity (G–L) for case A. L and R refer to the left and right measurement ports, respectively

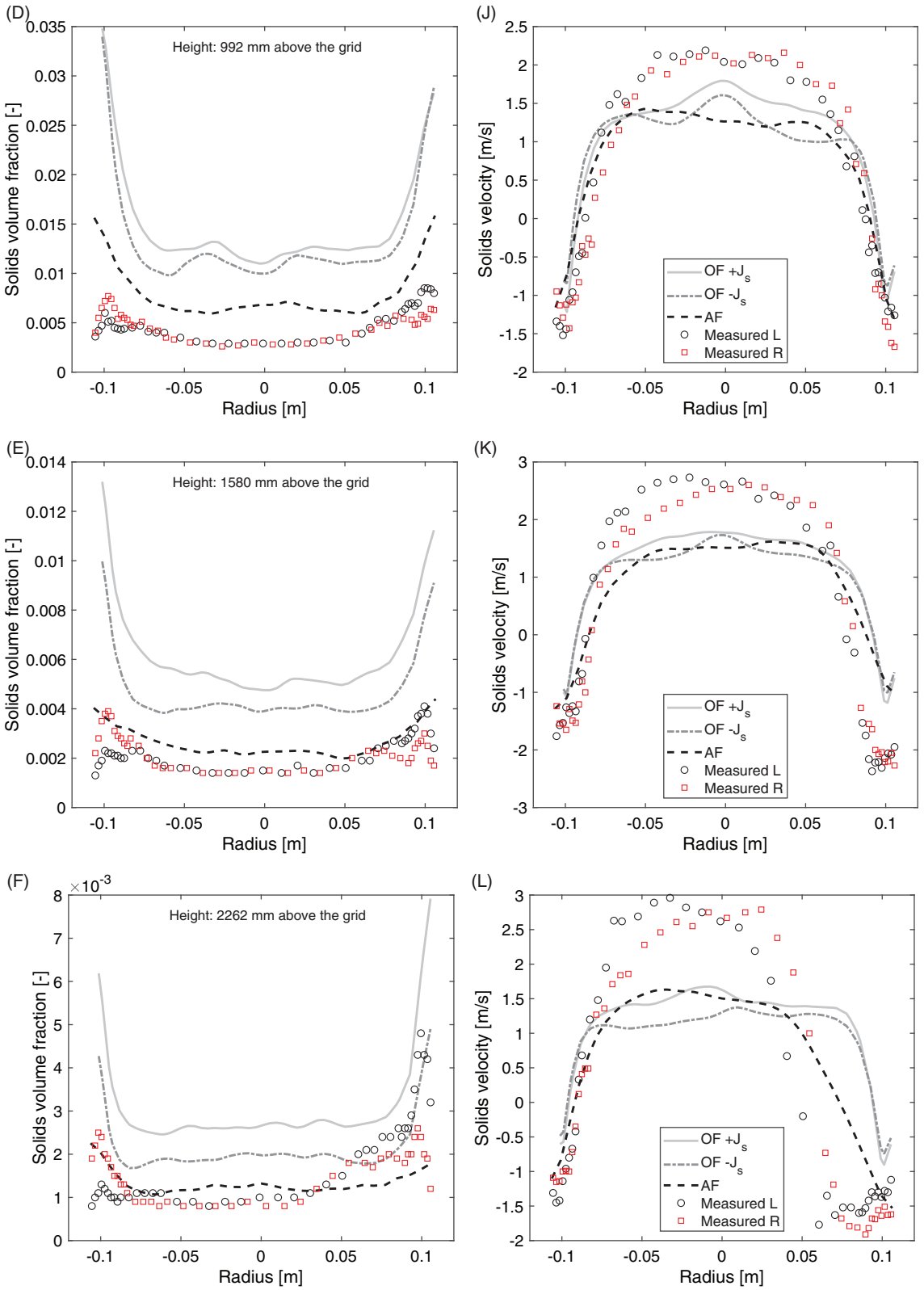

FIGURE 8 (Continued)

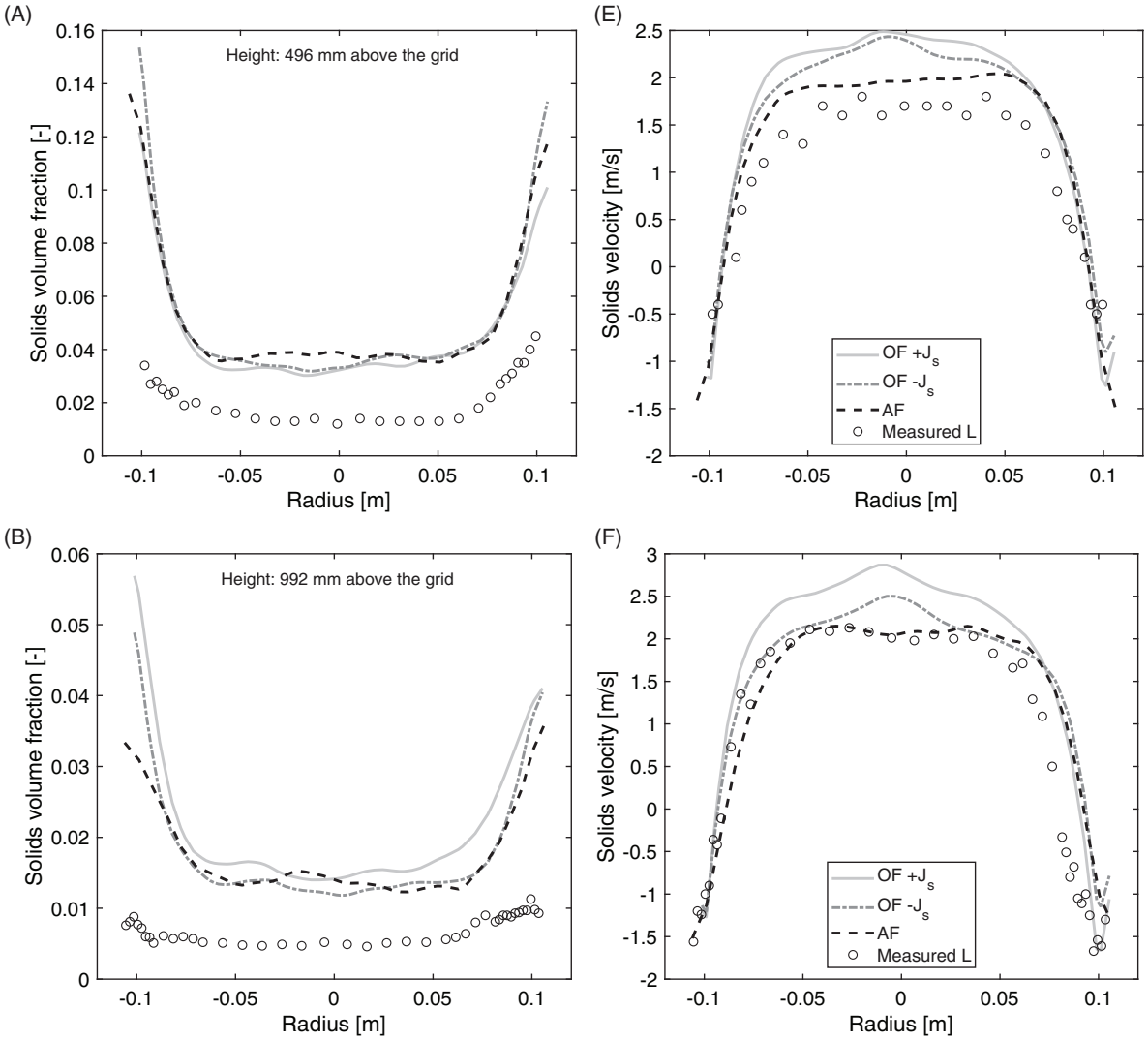

FIGURE 9 Profiles of solids volume fraction (A–D) and vertical velocity (E–H) for case B. L and R refer to the left and right measurement ports, respectively

all heights and the original OpenFOAM results separate clearly at 1580 mm level (C) instead of 992 mm level (B) as in case A.

4.2.5 | Effect of boundary conditions

The effect of boundary conditions was investigated in case A with the 10 mm mesh. The results are presented in Figures 10 and 11.

Comparison of the results with different boundary conditions indicates similar findings as with the pseudo-2D geometry, the differences between different boundary conditions with OpenFOAM are negligible, while there is a noticeable difference in Ansys Fluent results, which are discussed below. Contrary to the pseudo-2D results, the levels of solids volume fraction and velocity in the lower parts of the riser (Figure 11A,D) are similar between the boundary conditions, with larger differences becoming noticeable above 496 mm level. The free slip boundary condition produces consistently the lowest solids concentrations and velocities, and thus producing almost 40% lower recirculation rates than the Johnson–Jackson boundary conditions. The Johnson–Jackson and no slip boundary conditions predict similar velocities while the solids concentrations are higher with no slip, resulting in 20% higher recirculation rates.

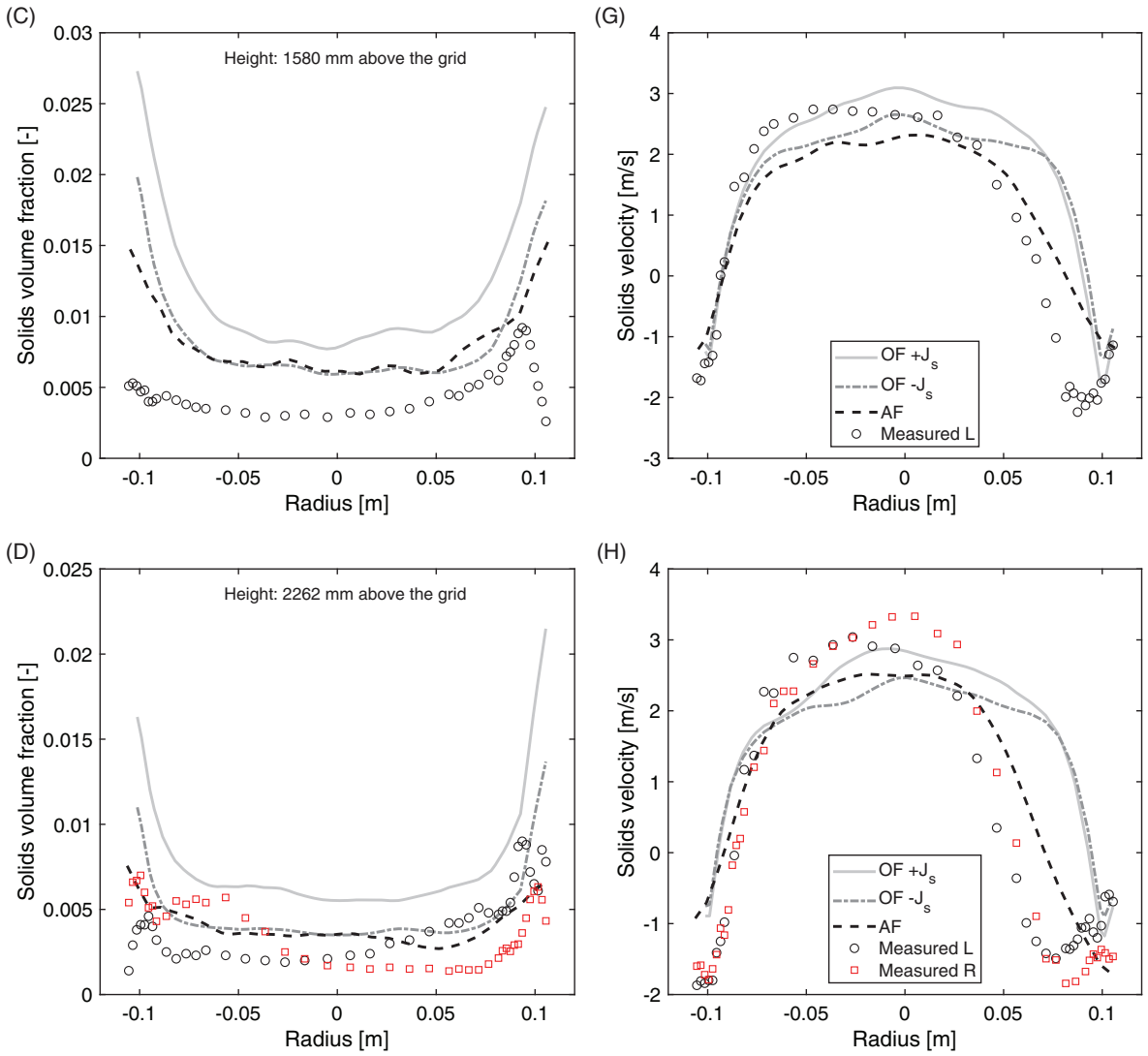

FIGURE 9 (Continued)

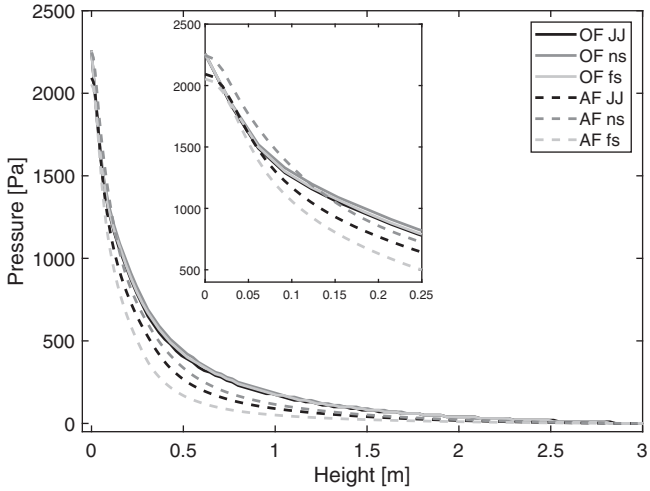

FIGURE 10 Comparison pressure profiles on the case A with (JJ) the Johnson–Jackson, no slip (ns), and free slip (fs) boundary conditions

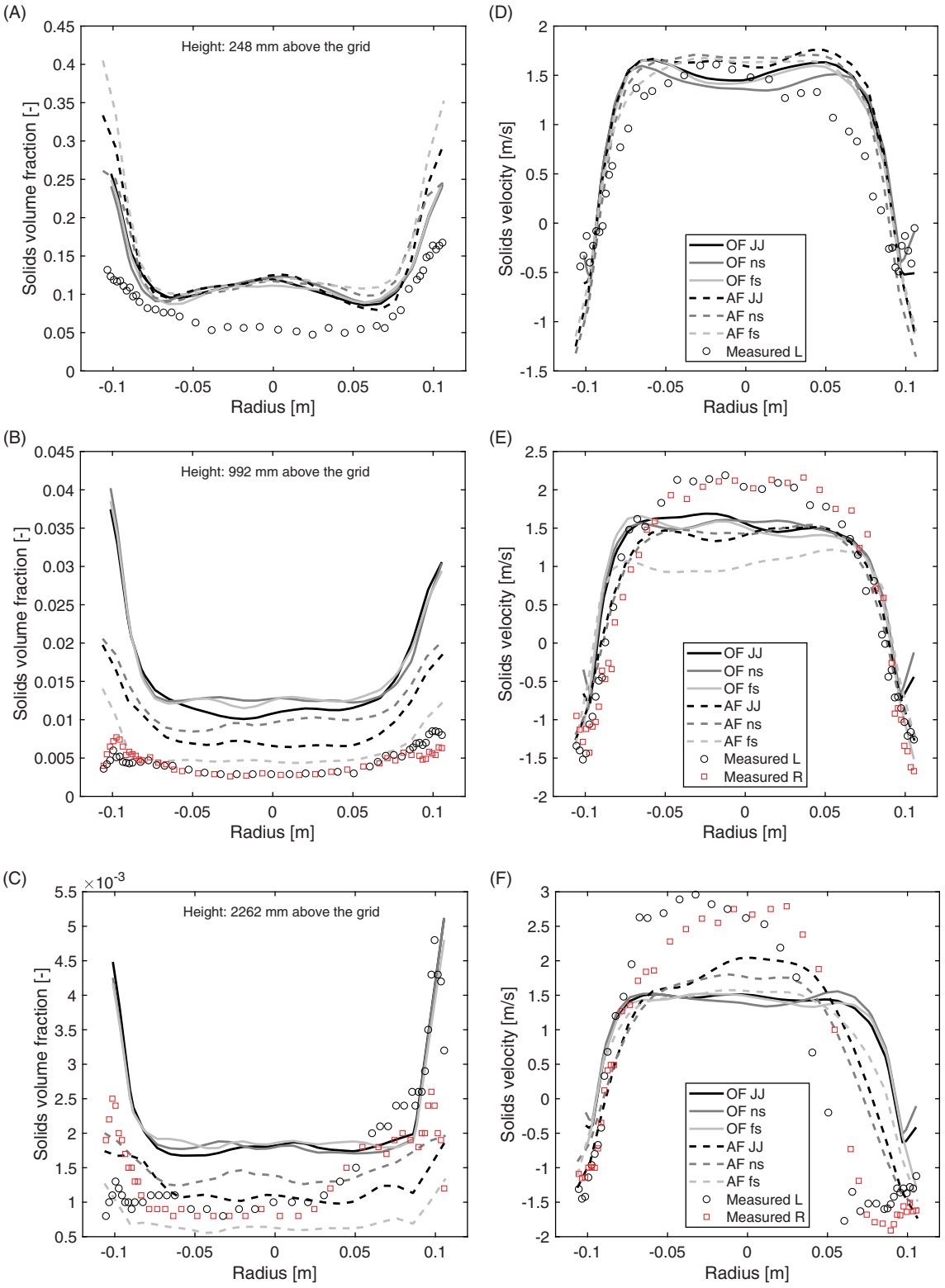

FIGURE 11 Comparison of profiles of solids volume fraction (A–C) and vertical velocity (D–F) in case A with (JJ) the Johnson–Jackson, no slip (ns), and free slip (fs) boundary conditions

5 | DISCUSSION

With the pseudo-2D riser, no significant differences were observed between the modified and original OpenFOAM formulation results. Reasons for this could be related to other parameters such as wall friction that is significant in a pseudo-2D unit, and collisional forces to walls. These effects can dominate over smaller terms such as the granular energy source terms where the modification was realized. In the cylindrical riser, where the effect of walls is smaller, the modified formulation of the granular energy equation in OpenFOAM reduced the levels of solids volume fraction and solids velocity in the riser, especially higher in the riser where the solids volume fraction is low. In the denser regions of the bottom and middle parts of the riser, the modification of the OpenFOAM formulation did not appear to have a significant effect on the observed measurement quantities. Immediately below the riser exit, almost an order of magnitude lower levels of average solids volume fraction were observed with Ansys Fluent and the modified OpenFOAM compared to the original OpenFOAM formulation. Ansys Fluent produces almost twice the axial solids velocities obtained with the two OpenFOAM versions, which predicted almost identical velocities. These two facts combined explain the level of mass flow rates in the external circulation. When the fluidization velocity was increased from 1.9 to 2.3 m/s, the modified OpenFOAM results increased their resemblance with Ansys Fluent results. This indicates that the operational parameter, such as the fluidization velocity and geometry (as seen in the pseudo-2D unit), affect the predictions of the software differently, and that the reason for this behavior is not solely the different source terms in the granular energy equation.

The effect of boundary conditions, that is, Johnson–Jackson, free slip, and no slip, seems to depend on the case and software, with negligible effects observed in OpenFOAM results, while Ansys Fluent results had noticeable differences. Ansys Fluent behaved differently on the pseudo-2D and cylindrical riser cases in terms of the region affected by the boundary conditions, with the lower part of the riser showing differences with the pseudo-2D riser and the upper part with the cylindrical riser. This behavior is difficult to explain, but it can be speculated that the effect of the walls in the pseudo-2D device is emphasizing the effect of the boundary conditions. The fluidization state is also more of a turbulent bed, thus the effects could be limited to the lower riser and above 1 m the results converge. On the cylindrical device, the effect of the walls is low compared to the particle interaction and the effect of the boundary conditions only becomes apparent higher in the riser in dilute conditions. The results indicate that Ansys Fluent is more sensitive to the selected boundary conditions and that the implementation of the Johnson–Jackson boundary condition does not explain the differences observed between the software results.

The granular temperatures of the systems were also investigated as a possible explanation for the observed differences, as the modification in OpenFOAM removed an additional positive source term from the conservation equation of the granular temperature. The expectation was that the granular temperature in the riser would be reduced and that the granular temperatures of the modified OpenFOAM would be more similar to Ansys Fluent results than the original OpenFOAM results. While the granular temperature levels dropped with the modification as was expected, it was found that Ansys Fluent had significantly higher levels of granular temperature compared to both OpenFOAM cases. Thus, by changing the granular temperature formulation of OpenFOAM to correspond with Ansys Fluent, the differences in granular temperature increased between Ansys Fluent and the modified OpenFOAM, while the measured simulation results (solids volume fraction, velocity, circulation mass flow rate) differences were reduced. No clear explanation for this unexpected result can be provided.

Granular temperature is directly influencing and influenced by many terms, such as granular pressure and volume fraction, as well as indirectly by a radial distribution function, restitution coefficient, viscosity terms, momentum exchange between phases and slip velocity. Therefore, it is difficult to say whether differences in observed time-averaged granular temperature levels are a cause or an effect. Logically, lowering of granular temperature in OpenFOAM leads to lower recirculation, since the granular pressure is proportional to the granular temperature, and lower granular pressure allows for denser packing and increases clustering. Given this, it would be expected that Ansys Fluent should have clearly a lower amount of packing and higher levels of recirculation, but this is not the case. This further indicates that source terms in the granular energy equation are not the cause for the differences in the results between the software.

The implementations of model and solution algorithms may contain (nonlinear) numerical limiters, which can mask out the differences in the solution variables such as granular temperature and that the differences in results are at least partly produced by such limiters. As an example of such a limiter, in OpenFOAM is the maximum value of viscosity is limited to 1000 by default to avoid numerical problems as the frictional viscosity is unbounded when the velocity gradients vanish. Similar limiters could be applied to granular and frictional pressures which, depending on the chosen models, can also be unbounded. When this type of limiter is active, the underlying models and values may not matter as the behavior

of the variable is dictated by the limiter. In Ansys Fluent the use of limiters is not reported in the documentation, but due to the numerical nature of the problem, some form of limitation must be used for stability.

Besides intentional limiters, unintentional implementation mistakes could explain the differences in the results. All multipurpose CFD software are quite complex, and it is possible that there are unnoticed implementation details or bugs which can significantly affect the results. Thus, although the OpenFOAM source code is publicly available, it can still contain bugs and implementation features that are not recognized. Ansys Fluent source code is not available and the exact implementation details are unknown. To get to the root cause of differences, a comprehensive verification study with a set of numerical experiments (preferably with analytical solutions) would need to be performed to evaluate when the software results start to differ from each other and possibly from other comparable CFD software.

6 | CONCLUSIONS

In this article, the effect of the two CFD software (using the same models, methods, and mesh) on the simulation results was studied in two circulating fluidized beds in turbulent bed and CFB conditions, compared to the previous studies of Herzog et al.[11] and Venier et al.[35] on bubbling fluidized beds. A difference in the formulation of the granular temperature source term between OpenFOAM and Ansys Fluent was recognized, modified to match, and the effect of the modification was investigated. While the modification reduced the differences between the software, significant differences still remained. The largest differences were observed in the bed material distribution, apparent in the pressure profile, external circulation mass flow rates, and the profiles of volume fraction. The vertical velocity profiles of the bed material also showed differences. An effort was made to investigate the possible reasons that could cause the differences in the results between the software. Johnson–Jackson, no slip, and free slip boundary conditions were tested and found not to be the source for the differences. An obvious difference was observed as Ansys Fluent had a higher overall level of granular temperature.

Unfortunately, it is not possible to confirm that the implementation of the models matched the reported or how the numerical methods are applied in Ansys Fluent, thus the source for these differences cannot be definitively recognized. Trusting the reporting of the models and their equations, the differences are likely implementation-based. The origins of the differences become important in cases where one software is used for model development and validation, after which the model is applied in another software, where the model results could vary significantly and even appear invalid.

Despite their differences, both software can produce reasonable results compared with the measurements, though each software predicts some aspects of the process better than the other. In general, Ansys Fluent exhibited better agreement with the measured pressure profile and solids volume fractions, while OpenFOAM better predicted the external circulation mass flow rates and solids velocities. Based on the available data it is not possible to claim that one of the software would be more accurate for fluidized bed modeling, both predicted the general behavior reasonably well and each had its strengths when compared with the available measurements. This research indicates that the simulated case, in addition to chosen models and boundary conditions, could affect the conclusion. While in some cases the software could produce equally accurate results, in other cases there could be large differences, and which software is considered better could vary with the case and model selection. More research comparing two or more software is needed along with detailed measurements in multiple CFB units with different flow conditions and materials as the results were observed to change in different risers and at different fluidization velocities.

ACKNOWLEDGMENT
This research did not receive any specific grant from funding agencies in the public, commercial, or not-for-profit sectors.

PEER REVIEW
The peer review history for this article is available at https://publons.com/publon/10.1002/eng2.12460.

DATA AVAILABILITY STATEMENT
The additional data that support the findings of this study are available from the authors upon reasonable request.

CONFLICT OF INTEREST
The authors have no conflict of interest relevant to this article.

AUTHOR CONTRIBUTIONS

Markku Nikku: Conceptualization (lead); formal analysis (equal); investigation (equal); methodology (equal); software (equal); visualization (equal); writing – original draft (lead); writing – review and editing (equal). **Timo Niemi:** Formal analysis (equal); investigation (equal); methodology (equal); software (equal); visualization (equal); writing – original draft (supporting); writing – review and editing (equal). **Sirpa Kallio:** Methodology (supporting); supervision (lead); writing – original draft (supporting); writing – review and editing (supporting). **Alexander Daikeler:** Investigation (supporting); validation (lead).

NOTATION

SYMBOLS

A	constant	[−]
C_D	drag coefficient	[−]
d	diameter	[m]
e	coefficient of restitution	[−]
$\mathbf{F}$	force	[N]
Fr	constant	[Pa]
$\mathbf{g}$	gravitational acceleration	[m s^{-2}]
g_0	radial distribution function	[−]
I_{2D}	second invariant of the deviator of the strain rate tensor	[s^{-2}]
J	fluctuating velocity/force correlation	[kg m^{-3} s^{-1}]
K	momentum exchange coefficient	[kg m^{-3} s^{-1}]
k	solids thermal conductivity	[kg m^{-1} s^{-1}]
p	pressure	[Pa]
Re	Reynolds number	[−]
S	source term	[kg s^{-1} or Pa]
t	time	[s]
u	vector velocity	[m/s]
α	volume fraction	[−]
γ	dissipation of granular energy	[kg m^{-3} s^{-1}]
θ	granular temperature	[m^2 s^{-2}]
λ	bulk viscosity	[Pa s]
μ	viscosity	[kg s^{-1} m^{-1}]
ρ	density	[kg m^{-3}]
τ	shear stress	[Pa]
ϕ	angle of internal friction	[°]

SUBSCRIPTS

col	collisional
fr	frictional
g	gas
kin	kinetic
m	momentum
max	maximum
rgh	hydrodynamic
s	solid
ss	solid–solid

ORCID

Markku Nikku https://orcid.org/0000-0001-5418-5328

REFERENCES

1. Nikku M, Myöhänen K, Ritvanen J, Hyppänen T, Lyytikäinen M. Three-dimensional modeling of biomass fuel flow in a circulating fluidized bed furnace with an experimentally derived momentum exchange model. *Chem Eng Res des*. 2016;115:77–90.

2. Gidaspow D. *Multiphase Flow and Fluidization: Continuum and Kinetic Theory Descriptions*. Academic Press; 1994.
3. Jianmin D, Gidaspow D. A bubbling fluidization model using kinetic theory of granular flow. *AIChE J*. 1990;36:523-538.
4. Gidaspow D, Bezburuah R, Ding J. Hydrodynamics of circulating fluidized beds: kinetic theory approach. In: Potter OE, Nicklin DJ, eds. *The Proceedings of the 7th Engineering Foundation Conference on Fluidization*. Engineering Foundation; 1992:75-82.
5. Ansys Fluent 19.1; 2018; Ansys Inc.
6. Ansys CFX 19.1; 2018; Ansys Inc.
7. Snider DM, O'Rourke PJ, Andrews MJ. Sediment flow in inclined vessels calculated using a multiphase particle-in-cell model for dense particle flows. *Int J Multiph Flow*. 1998;24:1359-1382.
8. Thapa RK, Frohner A, Tondl G, Pfeifer C, Halvorsen BM. Circulating fluidized bed combustion reactor: computational particle fluid dynamic model validation and gas feed position optimization. *Comput Chem Eng*. 2016;92:180-188.
9. Syamlal M, Rogers W, O'Brien T. MFIX documentation: theory guide; 1993.
10. NETL NETL multiphase flow science; 2018. Accessed 15th June 2018. https://mfix.netl.doe.gov/
11. Herzog N, Schreiber M, Egbers C, Krautz HJ. A comparative study of different CFD-codes for numerical simulation of gas–solid fluidized bed hydrodynamics. *Comput Chem Eng*. 2012;39:41-46.
12. The OpenFOAM Foundation Ltd The OpenFOAM foundation; 2018. Accessed June 15, 2018. https://openfoam.org/
13. Weller HG, Tabor G, Jasak H, Fureby C. A tensorial approach to computational continuum mechanics using object-oriented techniques. *Comput Phys*. 1998;12:620-631.
14. Liu Y, Hinrichsen O. CFD modeling of bubbling fluidized beds using OpenFOAM®: model validation and comparison of TVD differencing schemes. *Comput Chem Eng*. 2014;69:75-88.
15. ASCOMP TransAT CFD suite; 2018. Accessed June 15, 2018. http://ascomp.ch/products/transat-suite/
16. Tandon MP, Karnik AU. Simulation of rectangular fluidized bed with Geldart D particles. Paper presented at: Proceedings of 10th International Conference on CFD in Oil & Gas, Metallurgical and Process Industries SINTEF, 2014.
17. Runschke, E., Cancarevic, Z. & Schiephake, H. A CFD study of particle-laden flow of a Tundish water-model. Proceedings of the STAR Global Conference; 2014.
18. Ricklick M, Baran O. Analytical scaling of DEM particles for efficient packed-bed simulations. Proceedings of 10th International Conference on Heat Transfer, Fluid Mechanics and Thermodynamics HEFAT2014; 2014.
19. Panday R. Challenge problem: 1. model validation of circulating fluidized beds. *Powder Technol*. 2014;258:370-391.
20. Zhong W, Xie J, Shao Y, Liu X, Jin B. Three-dimensional modeling of olive cake combustion in CFB. *Appl Therm Eng*. 2015;88:322-333.
21. Wang Q. Particle size distribution in CPFD modeling of gas–solid flows in a CFB riser. *Particuology*. 2015;21:107-117.
22. Niemi T. Particle size distribution in CFD simulation of gas-particle flows. Diss. 2012;79:84.
23. Shi X, Wu Y, Lan X, Liu F, Gao J. Effects of the riser exit geometries on the hydrodynamics and solids back-mixing in CFB risers: 3D simulation using CPFD approach. *Powder Technol*. 2015;284:130-142.
24. Zhang W, You C. Numerical simulation of particulate flows in CFB riser with drag corrections based on particle distribution characterization. *Chem Eng J*. 2016;303:145-155.
25. Zeneli M, Nikolopoulos A, Nikolopoulos N, Grammelis P, Kakaras E. Application of an advanced coupled EMMS-TFM model to a pilot scale CFB carbonator. *Chem Eng Sci*. 2015;138:482-498.
26. Almuttahar A, Taghipour F. Computational fluid dynamics of high density circulating fluidized bed riser: study of modeling parameters. *Powder Technol*. 2008;185:11-23.
27. Zhou X, Gao J, Xu C, Lan X. Effect of wall boundary condition on CFD simulation of CFB risers. *Particuology*. 2013;11:556-565.
28. Kong L, Zhang C, Zhu J. Evaluation of the effect of wall boundary conditions on numerical simulations of circulating fluidized beds. *Particuology*. 2014;13:114-123.
29. Du S, Liu L. A local cluster-structure-dependent drag model for Eulerian simulation of gas-solid flow in CFB risers. *Chem Eng J*. 2019;368:687-699.
30. Zhu LT, Rashid TAB, Luo ZH. Comprehensive validation analysis of sub-grid drag and wall corrections for coarse-grid two-fluid modeling. *Chem Eng Sci*. 2019;196:478-492.
31. Upadhyay M, Park JH. CFD simulation via conventional two-fluid model of a circulating fluidized bed riser: influence of models and model parameters on hydrodynamic behavior. *Powder Technol*. 2015;272:260-268.
32. MacKenzie A, Lopez A, Ritos K, Stickland MT, Dempster WM. A comparison of CFD software packages' ability to model a surmerged jet. Proceedings of the 11th International Conference on CFD in the Minerals and Process Industries; 2015.
33. López A, Nicholls W, Stickland MT, Dempster WM. CFD study of jet impingement test erosion using ansys fluent® and OpenFOAM®. *Comput Phys Commun*. 2015;197:88-95.
34. Balogh M, Parente A, Benocci C. RANS simulation of ABL flow over complex terrains applying an enhanced k-ε model and wall function formulation: implementation and comparison for fluent and OpenFOAM. *J Wind Eng Ind Aerodyn*. 2012;104–106:360-368.
35. Venier CM, Reyes Urrutia A, Capossio JP, Baeyens J, Mazza G. Comparing ANSYS fluent® and OpenFOAM® simulations of Geldart a, B and D bubbling fluidized bed hydrodynamics. *Int J Numer Methods Heat Fluid Flow*. 2020;30:93-118.
36. Rusche H. *Computational Fluid Dynamics of Dispersed Two-Phase Flows at High Phase Fractions*. Imperial College, University of London; 2002.
37. Peltola J. *Dynamics in a Circulating Fluidized Bed: Experimental and Numerical Study*. Tampere University of Technology; 2009.
38. Mondal DN, Kallio S, Saxén H. Length scales of solid clusters in a two-dimensional circulating fluidized bed of Geldart B particles. *Powder Technol*. 2015;269:207-218.

39. Bi H, Fan L. Existence of turbulent regime in gas-solid fluidization. *AIChE J*. 1992;38:297-301.
40. Peltola J, Kallio S, Honkanen M, Saarenrinne P. Image based measurement of particle phase Reynolds stresses in a laboratory scale circulating fluidized bed. Proceedings of the 7th International Conference on Multiphase Flow; 2010:1-9.
41. Daikeler A, Ströhle J, Epple B. Experimental flow structure analysis in a 1 MWth circulating fluidized bed pilot plant. *Chem Eng Sci*. 2018;195:921–934. https://doi.org/10.1016/J.CES.2018.10.037
42. Stroh A. Coarse grain 3D CFD-DEM simulation and validation with capacitance probe measurements in a circulating fluidized bed. *Chem Eng Sci*. 2018;196:37–53. https://doi.org/10.1016/J.CES.2018.11.052
43. Nikku M, Daikeler A, Stroh A, Myöhänen K. Comparison of solid phase closure models in Eulerian-Eulerian simulations of a circulating fluidized bed riser. *Chem Eng Sci*. 2019;195:39-50.
44. Schaeffer DG. Instability in the evolution equations describing incompressible granular flow. *J Differ Equ*. 1987;66:19-50.
45. Lun CKK, Savage SB, Jeffrey DJ, Chepurniy N. Kinetic theories for granular flow: inelastic particles in couette flow and slightly inelastic particles in a general flow field. *J Fluid Mech*. 1984;140:223-256.
46. Johnson PC, Nott P, Jackson R. Frictional–collisional equations of motion for participate flows and their application to chutes. *J Fluid Mech*. 1990;210:501.
47. Ogawa S, Umemura A, Oshima N. On the equations for fluidized granular materials. *J Appl Math Phys*. 1980;31:483-493.
48. Sinclair JL, Jackson R. Gas-particle flow in a vertical pipe with particle-particle interactions. *AIChE J*. 1989;35:1473-1486.
49. van Wachem BGM, Schouten JC, van den Bleek CM, Krishna R, Sinclair JL. Comparative analysis of CFD models of dense gas-solid systems. *AIChE J*. 2001;47:1035-1051.
50. Louge MY, Mastorakos E, Jenkins JT. The role of particle collisions in pneumatic transport. *J Fluid Mech*. 1991;231:345-359.
51. Gidaspow, D., Bezburuah, R. & Ding, J. Hydrodynamics of circulating fluidized beds: kinetic theory approach. Proceedings of the 7th International Conference on Fluidization, Gold Coast (Australia); 1991.
52. Ergun S. Fluid flow through packed columns. *Chem Eng Prog*. 1952;48:89-94.
53. Wen CY, Yu YH. Mechanics of fluidization. *Chem Eng Prog Symp Ser*. 1966;62:100-111.
54. Vreman B, Geurts BJ, Deen NG, Kuipers JAM, Kuerten JGM. Two- and four-way coupled Euler–Lagrangian large-Eddy simulation of turbulent particle-Laden Channel flow. *Flow Turbul Combust*. 2009;82:47-71.
55. Helland E, Bournot H, Occelli R, Tadrist L. Drag reduction and cluster formation in a circulating fluidised bed. *Chem Eng Sci*. 2007;62:148-158.
56. Ansys ICEM CFD; 2016; Ansys Inc.
57. Kallio S, Peltola J, Niemi T. Analysis of the time-averaged gas-solid drag force based on data from transient 3D CFD simulations of fluidized beds. *Powder Technol*. 2015;274:227-238.
58. Johnson PC, Jackson R. Frictional–collisional constitutive relations for granular materials, with application to plane shearing. *J Fluid Mech*. 1987;176:67.

SUPPORTING INFORMATION

Additional supporting information may be found online in the Supporting Information section at the end of this article.

How to cite this article: Nikku M, Niemi T, Kallio S, Daikeler A. Effect of software implementation on the result of computational fluid dynamics simulation of circulating fluidized bed risers. *Engineering Reports*. 2021;e12460. https://doi.org/10.1002/eng2.12460